

# The Novel Oncolytic Adenoviral Mutant Ad5-3Δ-A20T Retargeted to αvβ6 Integrins Efficiently Eliminates Pancreatic Cancer Cells

Y. K. Stella Man<sup>1</sup>, James A. Davies<sup>2</sup>, Lynda Coughlan<sup>3</sup>, Constantia Pantelidou<sup>4</sup>, Alfonso Blázquez-Moreno<sup>5</sup>, John F. Marshall<sup>6</sup>, Alan L. Parker<sup>2</sup>, and Gunnel Halldén<sup>1</sup>

## Abstract

Metastatic pancreatic ductal adenocarcinomas (PDAC) are incurable due to the rapid development of resistance to all current therapeutics. Oncolytic adenoviral mutants have emerged as a promising new strategy that negates such resistance. In contrast to normal tissue, the majority of PDACs express the αvβ6 integrin receptor. To exploit this feature, we modified our previously reported oncolytic adenovirus, AdΔΔ, to selectively target αvβ6 integrins to facilitate systemic delivery. Structural modifications to AdΔΔ include the expression of the small but potent αvβ6-binding peptide, A20FMDV2, and ablation of binding to the native coxsackie and adenovirus receptor (CAR) within the fiber knob region. The resultant mutant, Ad5-3Δ-A20T, infected and killed αvβ6 integrin-expressing cells more effectively than the parental wild-type (Ad5wt) virus and AdΔΔ. Viral uptake through

αvβ6 integrins rather than native viral receptors (CAR, αvβ3 and αvβ5 integrins) promoted viral propagation and spread. Superior efficacy of Ad5-3Δ-A20T compared with Ad5wt was demonstrated in 3D organotypic cocultures, and similar potency between the two viruses was observed in Suit-2 *in vivo* models. Importantly, Ad5-3Δ-A20T infected pancreatic stellate cells at low levels, which may further facilitate viral spread and cancer cell elimination either as a single agent or in combination with the chemotherapy drug, gemcitabine. We demonstrate that Ad5-3Δ-A20T is highly selective for αvβ6 integrin-expressing pancreatic cancer cells, and with further development, this new and exciting strategy can potentially be extended to improve the systemic delivery of adenoviruses to pancreatic cancer patients. *Mol Cancer Ther*; 17(2); 575–87. ©2018 AACR.

## Introduction

Pancreatic ductal adenocarcinomas (PDAC) are aggressive cancers with high mortality and low 5-year survival rates globally (1). Major reasons for the dismal prognosis are the late presentation of symptoms and the rapid development of resistance to all current therapeutics that do not significantly prolong survival (1, 2). Replication-selective oncolytic adenoviruses efficiently target all epithelial cancers, including treatment-resistant pancreatic cancer cells, and have excellent safety records in early-phase clinical trials. The first oncolytic adenoviral mutant to be evaluated in pancreatic cancer patients was

Onyx-015 (*dl1520*) with deletion of the E1B55K gene enabling virus propagation in cancer cells with aberrant nuclear mRNA export and nonfunctional p53 (3–5). Despite proven safety in two phase I trials in conjunction with gemcitabine, efficacy was limited because essential viral functions were compromised by the deletion. More recently, mutants with higher efficacy have been developed by deleting the small pRb-binding E1ACR2-region (ΔCR2) that prevent replication in normal tissue, while viral propagation and spread in tumor cells is complemented by deregulated cell-cycle control (pRb-p16 regulation; refs. 6–8). The most common genetic alterations in pancreatic cancer are activating *KRAS* mutations, *CDKN2A/p16* deletion, and inactivating *TP53* mutations (9) and consequently, replication of E1ΔCR2 mutants readily proceeds. E1ΔCR2 mutants have not yet been evaluated in PDAC patients, while promising outcomes were reported in gliomas and osteosarcomas with Ad5ΔCR2 variants (8, 10).

We recently developed the novel mutant AdΔΔ with the anti-apoptotic E1B19K gene deleted in addition to the E1ACR2 deletion (6, 11, 12). E1B19K is a functional Bcl-2 homolog that binds Bax and Bak and inhibits mitochondrial pore formation and apoptosis in response to death receptor activation and intrinsically induced apoptosis (13). AdΔΔ synergized with the current clinical standard of care for pancreatic cancer, gemcitabine and irinotecan, without toxicity to normal cells (6, 11, 14). However, to efficiently target pancreatic cancer lesions in patients by systemic administration required further modifications. Human erythrocytes express high levels of the native viral receptor, coxsackie and adenovirus receptor (CAR) and complement receptor

<sup>1</sup>Centre for Molecular Oncology, Barts Cancer Institute, Queen Mary University of London, United Kingdom. <sup>2</sup>Division of Cancer and Genetics, School of Medicine, Cardiff University, Cardiff, United Kingdom. <sup>3</sup>Department of Microbiology, Icahn School of Medicine at Mount Sinai, New York, New York. <sup>4</sup>Medical Oncology, Dana Farber Cancer Institute, Boston, Massachusetts. <sup>5</sup>Department of Immunology and Oncology, Centro Nacional de Biotecnología-Consejo Superior de Investigaciones Científicas, Madrid, Spain. <sup>6</sup>Centre for Tumour Biology, Barts Cancer Institute, Queen Mary University of London, United Kingdom.

**Note:** Supplementary data for this article are available at Molecular Cancer Therapeutics Online (<http://mct.aacrjournals.org/>).

**Corresponding Author:** Gunnel Halldén, Barts Cancer Institute, a Cancer Research UK Centre of Excellence, Queen Mary University of London, London EC1M 6BQ, United Kingdom. Phone: 4420-7882-3593; Fax: 4420-7882-3884; E-mail: g.hallden@qmul.ac.uk

**doi:** 10.1158/1535-7163.MCT-17-0671

©2018 American Association for Cancer Research.

1 (CR-1) that bind the viral fiber knob in the presence of neutralizing antibodies and complement, resulting in lower doses of virus reaching the tumor (15). Other barriers to systemic delivery are the rapid elimination of virus by hepatic Kupffer cells and hepatocyte uptake, and the high-affinity binding to numerous blood factors (16–18). For example, factor X binds to the viral hexon protein and bridges the virus to heparan sulfate proteoglycans mainly on the hepatocyte surface and promotes liver transduction (17). Factor IX (FIX) has also been reported to aid the transduction of hepatocytes, although it remains unclear which viral protein is responsible, and complement-4-binding protein (C4BP) binds to the fiber knob (16, 18). Importantly, viral binding to blood factors rapidly induces innate immune activation to the vector, resulting in systemic inflammatory responses in patients (18, 19). We hypothesized that the local viral concentration at tumor sites could be increased by: (i) targeting of mutants to pancreatic tumors and (ii) decreasing binding to erythrocytes and blood factors. Ultimately, we generated a novel oncolytic adenovirus modified to improve tumor targeting.

The  $\alpha v\beta 6$  integrin is highly expressed in many solid tumors but not in normal cells (20–22). To take advantage of the selective expression of  $\alpha v\beta 6$  integrin in PDAC cells, we previously generated the retargeted wild-type mutants Ad5A20 and Ad5A20-477dITAYT (23, 24). The mutants were engineered to express a 20 amino acid peptide A20FMDV2 derived from the foot-and-mouth disease virus (FMDV) that selectively binds through an Arg-Gly-Asp (RGD)-domain to  $\alpha v\beta 6$  (25, 26). Ad5-A20477dITAYT was also modified to reduce CAR and complement binding and partially relieved some of the obstacles with systemic delivery by reducing erythrocyte binding (23, 24).

In this study, we report on the generation of a novel mutant, Ad5-3 $\Delta$ -A20T based on the oncolytic mutant Ad $\Delta\Delta$ , with incorporation of the A20FMDV2 peptide, ablation of CAR binding, and deletion of E3gp19K, for optimal replication-selectivity, cancer targeting, and immune stimulation. Ad5-3 $\Delta$ -A20T potently replicated in and killed cultured PDAC cells, in xenografts *in vivo* and in 3-dimensional (3D) coculture models with pancreatic stellate cells. Ad5-3 $\Delta$ -A20T was highly efficacious and retained all viral functions necessary for propagation in pancreatic cancer cells also in the presence of gemcitabine. We expect these findings to guide further optimization of oncolytic adenoviruses for systemic delivery to improve on therapeutic efficacy in patients with pancreatic cancer in conjunction with current treatments.

## Materials and Methods

### Cell lines and culture conditions

Human PDAC cell lines were used in the study: BxPC-3, Panc04.03, Capan-2, PANC-1, and MiaPaCa-2 (primary tumors); CFPAC-1 and Capan-1 (liver metastasis), Hs766t (lymph node metastasis) (ATCC, LGC Standards), and Suit-2, PaTu8902 and PaTu8988t (liver metastasis) and PaTu8988s (primary tumor) (Cell Services, Cancer Research UK). The PT45 cells (primary tumor) were a kind gift from Prof H. Kalthoff (Comprehensive Cancer, Campus Kiel, Kiel, Germany). The hTERT-immortalized human pancreatic stellate cells (PS1) were a kind gift from Prof. H. Kocher (BCI, QMUL, London, United Kingdom; ref. 27). The human embryonic kidney cells HEK293 and JH293 (Cell Services, Cancer Research UK) and the human lung carcinoma cells A549 (LGC Standards) were used for viral production. Cells were grown at 37°C and 5% CO<sub>2</sub> in DMEM supplemented with 10% FBS and

1% penicillin and streptomycin (penicillin 10,000 U/ml, streptomycin 10 mg/ml; P/S; Sigma-Aldrich). All cell lines were STR-profiled (LGC Standards and Cancer Research UK) and verified to be identical to the profiles reported by the suppliers and to the original vial.

### Organotypic 3D coculture models

The development of the 3-dimensional (3D) coculture models (organotypic cultures) for pancreatic adenocarcinoma cells and stromal cells has been previously described in detail elsewhere (27–29). Briefly, collagen type I was mixed with Matrigel at different ratios, typically 3:1, in Transwells (Corning; Sigma-Aldrich) and placed in 24-well plates. Panc0403 or Suit-2 cells were seeded together with PS1 cells (typical ratio 1:2; total  $1 \times 10^5$  cells/well) on top of gels in 10% FBS Ham's F12/DMEM (Gibco). After 24 hours, the media in the top chamber were replaced with serum-free DMEM; 3 to 4 days later, viruses were added at 2- to 5-fold higher doses than in regular 2D cultures and fixed in formalin 4 to 7 days later. In some studies, cells were embedded within the gels and virus added either in the top or bottom compartment. In combination studies, gemcitabine (Gemzar; Eli Lilly) was added at 5 to 10 nmol/L in serum-free DMEM on top of gel and/or in 10% FBS Ham's F12/DMEM underneath the transwell.

### Viruses and infections

Wild-type virus Ad5 and the modified EGFP-expressing mutants, Ad5, Ad5A20, and Ad5A20-477dITAYT were previously generated from species C wild-type adenovirus type 5 (23, 24). Briefly a 20-amino acid RGD-binding peptide (A20FMDV2; NAVPNLRGDLQVLAQKVART; ref. 26) from VP1 of the FMDV (30) was incorporated in the HI-loop of the Ad5 fiber knob in Ad5A20 (23). Ad5A20 was further modified to generate Ad5A20-477dITAYT through a base substitution Y477A and a deletion of amino acids 489–492 (TAYT) in the fiber knob, and the E3gp19K gene was replaced by EGFP (18, 24, 31). Generation of Ad $\Delta\Delta$  (deleted in E1ACR2 and E1B19K) has been described previously (6, 12). Ad5-3 $\Delta$ -A20477dITAYT (Ad5-3 $\Delta$ -A20T) was generated by two-step homologous recombination in SW102 bacteria (32, 33). The wild-type Ad5 genome previously captured within a bacterial artificial chromosome was modified in a series of stages (primer sequences; Supplementary Table S1). First, the wild-type E1 genes were replaced with the PCR-amplified modified E1-region from Ad $\Delta\Delta$ . Next, the fiber knob domain of Ad5A20-477dITAYT was PCR amplified and inserted to replace the wild-type knob. Finally, the E3gp19K domain was deleted generating Ad5-3 $\Delta$ -A20T. The viruses were produced, purified, and characterized according to standard protocols (6, 12). The viral particle (vp) to infectious unit [plaque-forming units (pfu)] was 9–45 vp/pfu for all viruses with the highest ratios for the FMDV-expressing mutants. All infections were performed in serum-free DMEM, and 2 hours later, the media were replaced with 10% FBS/1% P/S DMEM  $\pm$  the indicated doses of drugs.

### Cell viability assay

Cells were infected with viral mutants in 2% FBS/1% P/S DMEM and were assayed 72 or 96 hours later using the 3-(4,5-dimethylthiazol-2-yl)-5-(3-carboxymethoxyphenyl)-2-(4-sulfophenyl)-2H-tetrazolium assay (MTS; Promega) to quantify live cells as an indirect measurement of cell death. Dose-response curves were generated to determine the concentration of each

virus killing 50% of cells ( $EC_{50}$ ) using untreated cells as controls. Each data point was generated from triplicate samples and experiments repeated at least three times as described previously (12).

#### Viral genome amplification by qPCR

Cells were infected with 100 particles per cell (ppc) of the respective virus and were harvested 24, 48, and 72 hours later. The cell suspensions were pelleted, snap-frozen, and stored at  $-80^{\circ}\text{C}$ . DNA was extracted using the QIAamp DNA Blood Mini Kit, according to the manufacturer's instructions (Qiagen) and used for quantitative PCR (qPCR) analysis as described previously (11, 14).

#### Viral replication assay by tissue culture infectious dose ( $TCID_{50}$ )

Cells were infected as described for qPCR, and cells and media were collected at the indicated time points, freeze-thawed, and analyzed by the  $TCID_{50}$  limiting dilution method on JH293 or A549 cells. Ad5 wild-type virus of known activity was included in every assay as internal control as described previously (14).

#### Quantification of infectivity and cell surface receptor levels

Cells were seeded ( $1 \times 10^5$  cells/well) in 6-well plates 24 hours prior to infection with the EGFP-expressing mutants at 100 or 500 ppc in serum-free DMEM; 2 hours later, media were replaced with 10% FBS/DMEM. Viral infectivity was quantified by flow cytometry analysis (FACS) using EGFP expression as a marker, 48 and 72 hours postinfection. Cells were detached with trypsin/EDTA and combined with nonattached cells in the media and resuspended in cold FACS buffer (0.1% BSA/DMEM).

To quantify cell surface receptors, cells were grown and treated as described above, resuspended, and incubated on ice for 1 hour with the respective primary mouse mAb; anti-CAR (anti-CAR at 1:1,000; ATCC), anti- $\alpha v\beta 3$  integrin (1:100; Chemicon), anti- $\alpha v\beta 5$  (1:100; Cancer Research UK), and anti- $\alpha v\beta 6$  (1:100; Clone 10D5, Millipore). Bound antibodies were detected with secondary goat anti-mouse IgG conjugated to FITC (Alexa Flour 488 at 1:250; Molecular Probes) for 1 hour. To determine the role of each receptor, antibodies targeting  $\alpha v\beta 5$  or  $\alpha v\beta 6$  (at 1:100) or the A20FMDV2 peptide (10 nmol/L) were incubated with the cells for 10 minutes on ice prior to the addition of virus.

EGFP expression and cell surface protein levels were determined by detection of fluorescence on the FACSCalibur instrument acquiring 10,000 events per sample and analyzed using the FlowJo software 8.8.6 (Tree Star Inc.).

#### IHC

Formalin-fixed paraffin-embedded cells, organotypic cultures, or tissue sections (10  $\mu\text{m}$ ) were dewaxed, rehydrated in decreasing ethanol concentrations, water, and PBS. Antigen retrieval was performed by boiling in 10 mmol/L sodium citrate buffer pH6 for 8 minutes, followed by water and PBS at  $24^{\circ}\text{C}$ . Cell permeabilization was for 5 minutes in 0.2% Triton-X/PBS in blocking buffer (2% BSA/10% FBS/PBS). Primary antibodies,  $\alpha\text{SMA}$  (1:300; M0851, Dako), and E1A (1:500; M58, GeneTex) were incubated overnight at  $4^{\circ}\text{C}$ , followed by fluorescent-labeled secondary anti-mouse antibodies for 1 hour (1:500; Alexa Fluor 488, Thermo Fisher Scientific). Sections were stained with 4',6'-diamidino-2-phenylindole (DAPI, 1 mg/mL; Thermo Fisher Scientific), mounted with FluorSave Reagent (Calbiochem), stored at  $-20^{\circ}\text{C}$ , and analyzed by confocal microscopy (Zeiss 710).

Tumors were harvested at the end of the study and fixed in 4% formaldehyde. The fixed tissues were sectioned and processed for histopathology with hematoxylin and eosin (H&E) and for IHC by staining for E1A and hexon (1:2,000; Autogen Bioclear), followed by detection using HRP-conjugated secondary antibodies (Dako).

#### *In vivo* tumor growth

Tumor cells were inoculated subcutaneously in one flank of CDnu/nu athymic mice (Charles River Laboratories) with Suit-2 cells in sterile PBS ( $1 \times 10^6$  cells/200  $\mu\text{L}$ ). Treatments were initiated when tumor volumes reached  $100 \pm 20$   $\mu\text{L}$  (14 days after inoculation) by intratumoral administration of adenoviral mutants at doses ranging from  $1 \times 10^8$  to  $3 \times 10^9$  vp/injection, on day 1, 3, and 6 or day 1, 3, 5, 7, and 9. Tumor growth, progression, and animal weight were followed until tumors reached 1.44  $\text{cm}^2$  or until symptomatic tumor ulceration occurred (according to UK Home Office Regulations). Tumor volumes were estimated twice weekly: volume =  $(\text{length} \times \text{width}^2 \times \pi)/6$ , and growth curves were compared using one-way ANOVA. Survival analysis was performed according to the method of Kaplan–Meier (log-rank test for statistical significance). Each treatment group included 8 animals and studies were performed twice according to two protocols as described above. For viral distribution studies, virus was administered via the tail vein with a single injection of  $3 \times 10^9$  vp in 100  $\mu\text{L}$ . Tumors were harvested 24, 48, and 72 hours later, sonicated, and protein expression determined by Western blotting (Supplementary Materials and Methods). E1A was detected by mouse anti-E1A (1:500; M58, GeneTex) and PCNA by mouse anti-PCNA (1:1,000; Santa Cruz Biotechnology).

## Results

### Pancreatic cancer cells express higher levels of $\alpha v\beta 6$ integrin than CAR and are more susceptible to infection with A20FMDV2-retargeted mutants than with Adwt

Pancreatic tumors frequently express the  $\alpha v\beta 6$  integrin, reported to play a role in the progression of pancreatic cancer (21, 34). A panel of 15 human pancreatic cancer cell lines was screened for  $\alpha v\beta 6$  integrin expression to determine the feasibility of retargeting the replication-selective Ad $\Delta\Delta$  to this integrin. Expression levels were high in the majority of cell lines, while levels of the native adenovirus receptor CAR were consistently low compared with the JH293 cells (Fig. 1A; Supplementary Fig. S1A). The degree of infectivity with the FMDV2-expressing Ad5A20 (targeting  $\alpha v\beta 6$  and CAR) and Ad5A20-477dITAYT (targeting  $\alpha v\beta 6$  only) was markedly higher than with wild-type Ad5 (Ad5wt; targeting CAR only) across all cell lines that expressed the  $\alpha v\beta 6$  integrin (Fig. 1A and B; Supplementary Fig. S1B). Infection levels strongly correlated with  $\alpha v\beta 6$  integrin expression ( $R^2 = 0.7$ ; Fig. 1C). In contrast, no correlation was obtained between Ad5A20- or Ad5A20-477dITAYT-infection and CAR levels or between Ad5wt infection and  $\alpha v\beta 6$  integrin expression levels ( $R^2 \leq 0.2$ ; Supplementary Fig. S1C and S1D).

After the initial screening of 15 cell lines, we selected 5 of these for further in-depth studies that represented a range of  $\alpha v\beta 6$  integrin expression levels; PT45 low, Panc04.03 high, and MIA PaCa-2, Suit-2, and BxPC-3 intermediate (Fig. 1A). Infection in Suit-2 and Panc04.03 cells were significantly higher with Ad5A20

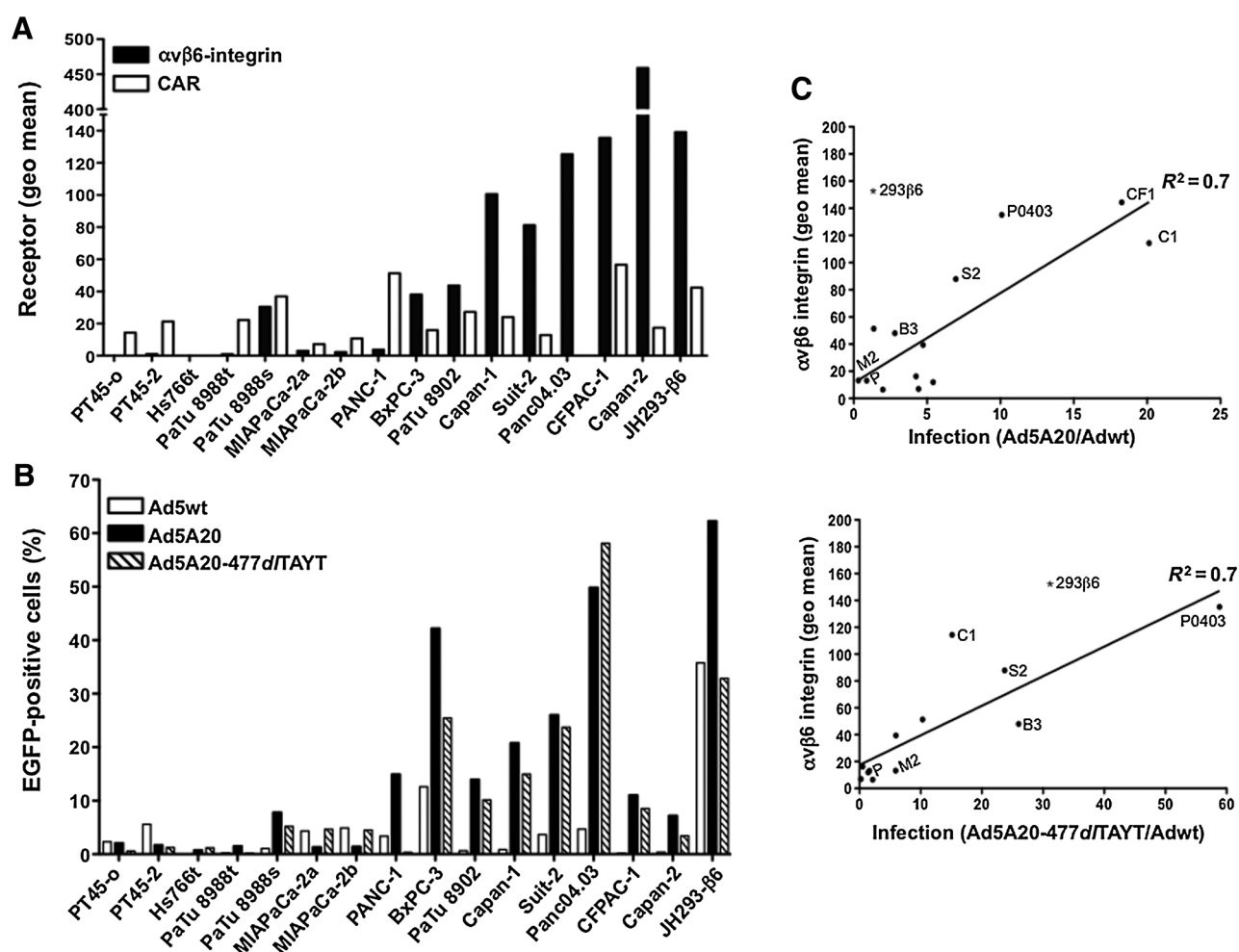


**Figure 1.**

Higher levels of  $\alpha v\beta 6$  integrin expression in pancreatic cancer cell lines support higher levels of infection with the retargeted A20FMDV2-expressing Ad5A20 and Ad5A20-477d/TAYT mutants. **A**, Fifteen pancreatic epithelial cancer cell lines were screened for expression of  $\alpha v\beta 6$  integrin and CAR. Cells were probed with  $\alpha v\beta 6$ - or CAR-specific antibodies, detected by flow cytometry and expression presented as geometric mean values, one representative study. **B**, Viral infectivity levels in the panel of cells were determined by flow cytometry. Cells were infected with Ad5wt, Ad5A20, and Ad5A20-477d/TAYT at 100 ppc, assay was performed 48 hours postinfection, and EGFP expression was quantified, one representative study. **C**, Correlation of data from studies performed as in **A** and **B**, for  $\alpha v\beta 6$  integrin expression and degree of infectivity of Ad5A20 (top) and Ad5A20-477d/TAYT (bottom). Viral infectivity is expressed as a ratio of that corresponding to Ad5wt, to isolate the effect on infectivity mediated by the  $\alpha v\beta 6$  integrin only.  $R^2$  values are displayed following linear regression analysis, one representative study out of three.

and Ad5A20-477d/TAYT compared with infection with Ad5wt ( $P < 0.05$ ; Suit-2 and  $P < 0.01$ ; Panc04.03; Fig. 2A). A similar trend was observed in BxPC-3 cells, while in MIA PaCa-2 or PT45 cells, all viruses infected to a similar degree. Infection levels in all five cell lines strongly correlated with the expression levels of  $\alpha v\beta 6$  integrin (Ad5A20,  $R^2 = 0.99$ ; Fig. 2B). The A20FMDV2-expressing mutants caused significantly higher levels of cell killing in Suit-2 and Panc04.03 cells compared with Ad5wt ( $P \leq 0.05$ ) but not in PT45, MIA PaCa-2a, or BxPC-3 (Fig. 2C). The BxPC-3 cells were the most sensitive to Adwt infection with the lowest  $EC_{50}$  values of all tested cell lines (Supplementary Table S2). Despite higher levels of infection with the retargeted Ad5A20/TAYT and Ad5A20 mutants in BxPC-3 cells (Fig. 2A), it is possible that the lower  $EC_{50}$  values for both Adwt and mutants masked small differences in cell killing ability in these cells.

#### Viral genome amplification is increased with A20FMDV2-expressing mutants in cells expressing high levels of the $\alpha v\beta 6$ integrin

In Suit-2 and Panc04.03 cells, the enhanced infection and cell killing with the A20FMDV2 mutants were paralleled by higher levels of viral genome amplification compared with infection with Ad5wt at all time points (24–72 hours; Fig. 2D). In agreement with the cell killing and infectivity data, Ad5wt genome amplification was greater in PT45 cells with a similar trend in MIA PaCa-2 cells cell. In BxPC-3 cells, all three viruses replicated to similar levels. In conclusion, variations in the absolute levels of genome amplification between Ad5wt and the retargeted mutants directly reflected the different levels of viral uptake (24-hour time point) for each cell line as a consequence of the increased number of viral genomes available after infection. In contrast, the relative

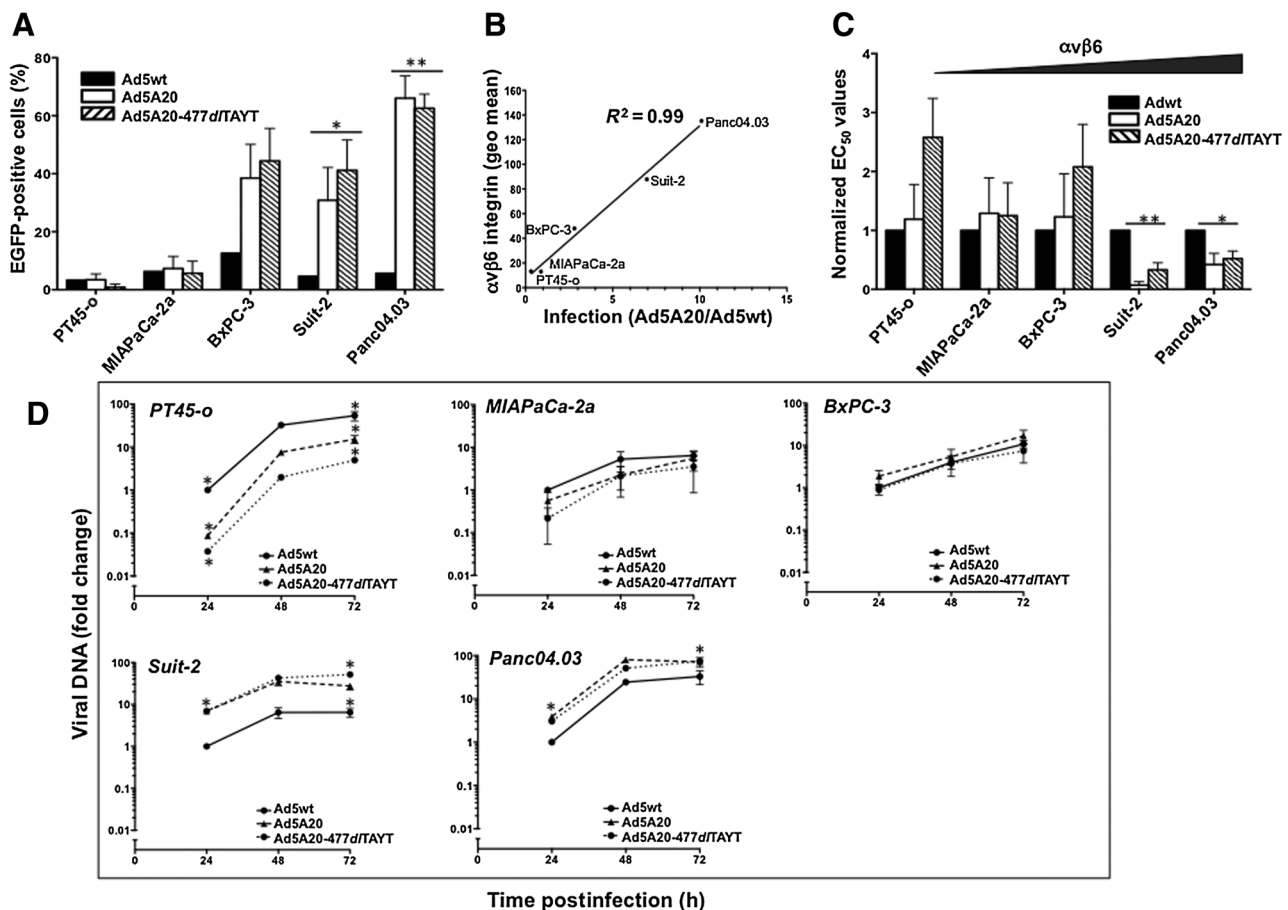


**Figure 2.**

The cell killing potency of Ad5A20 and Ad5A20-477dITAYT is significantly higher than that of Ad5wt in  $\alpha\beta 6$  integrin expressing pancreatic cancer cell lines. Five pancreatic cell lines spanning low to high expression levels of  $\alpha\beta 6$  integrin were selected for further studies. **A**, Cells were infected with Ad5wt, Ad5A20, and Ad5A20-477dITAYT at 100 ppc and infectivity quantified by flow cytometry via EGFP detection, 48 hours postinfection,  $n \geq 3$ . **B**, A strong correlation between  $\alpha\beta 6$  integrin expression and Ad5A20/Ad5wt was observed in the five cell lines ( $R^2 = 0.99$ ). **C**, For each cell line, viral dose-response curves were generated and cell viability was analyzed (MTS-assay) 72 hours postinfection. EC<sub>50</sub> values were determined for each virus and normalized to the EC<sub>50</sub> value of Ad5wt per cell line. The increasing  $\alpha\beta 6$  integrin expression levels are indicated on the graph. **A** and **C**, Error bars, SD,  $n \geq 3$ ,  $P < 0.05$ ;  $**$ ,  $P < 0.01$ , one-way ANOVA. **D**, Viral DNA replication was quantified by qPCR. Cells were infected (100 ppc) with the indicated viral mutant and harvested 24, 48, and 72 hours later. Results were compared among the three viruses by normalizing the values to that of Ad5wt at 24 hours and are expressed as fold change,  $n \geq 2$ ,  $P < 0.01$ , one-way ANOVA comparing mutant/Adwt at indicated time points and 72/24 hours.

replication rates of the retargeted mutants in individual cell lines remained similar to Ad5wt.

#### Blocking $\alpha\beta 6$ integrin attenuates infection with Ad5A20 and Ad5A20-477dITAYT but not with Ad5wt

The  $\alpha\beta 3$  and  $\alpha\beta 5$  integrins play a major role in internalization of Ad5wt, mediated by penton-integrin binding through RGD interactions. To examine whether these integrins were also essential for the FMDV-retargeted mutants or whether binding to the  $\alpha\beta 6$  integrin alone was sufficient for cellular uptake of virus, we first determined the expression levels of  $\alpha\beta 3$  and  $\alpha\beta 5$  integrins (Fig. 3A). PT45 and Suit2 cells expressed the highest levels of  $\alpha\beta 5$  integrins and BxPC-3 of the  $\alpha\beta 3$  integrin. The greatest expression of  $\alpha\beta 6$  integrins was observed in Suit-2 and Panc04.03 cells. Blocking of  $\alpha\beta 6$  integrin receptors with free A20FMDV2 peptide significantly decreased the infection levels with Ad5A20 and Ad5A20-477dITAYT but not with Ad5wt in

Panc04.03, Suit-2, and BxPC-3 cells (Fig. 3B). The most pronounced effect was in Suit-2 and Panc04.03 cells with reductions up to 70% compared with original levels of infection. Decreased E1A expression in cells infected with Ad5A20-477dITAYT but not with Ad5wt further confirmed our findings (Panc0403; Supplementary Fig. S1E). Thus, Ad5A20 and Ad5A20-477dITAYT were mainly internalized through  $\alpha\beta 6$  integrins in pancreatic cancer cells, although other integrins, such as  $\alpha\beta 5$ , may contribute toward the process. Importantly, in cells with low or nondetectable levels of  $\alpha\beta 6$  integrins, infection with the retargeted mutants was reduced compared with infection with Ad5wt (Figs. 3A and B and 1B).

#### Viral replication and spread is supported in organotypic 3D cocultures of pancreatic cancer and stromal cells

Pancreatic cancer cells (PDACs) *in situ* are typically embedded in a dense tumor-supporting fibrous stroma, with pancreatic

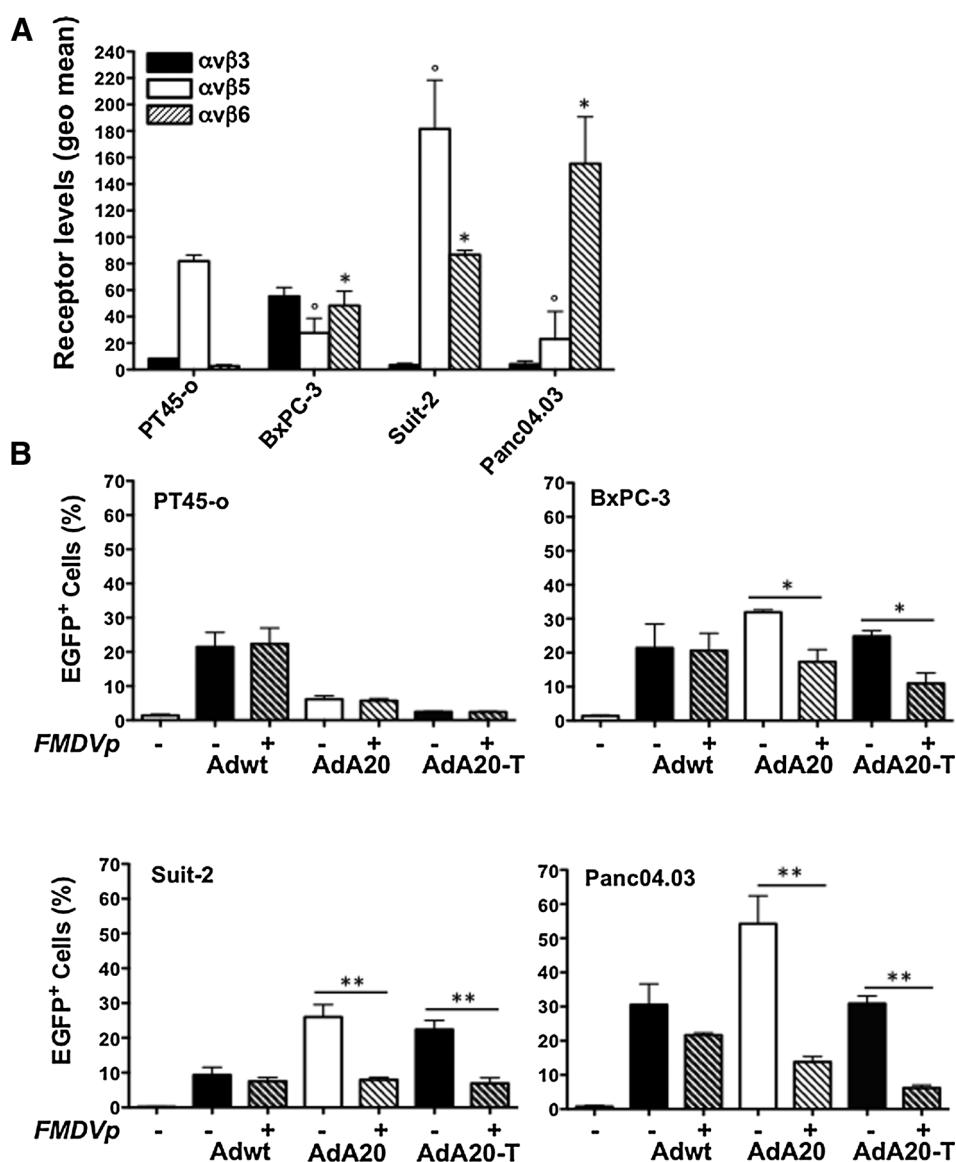


**Figure 3.**

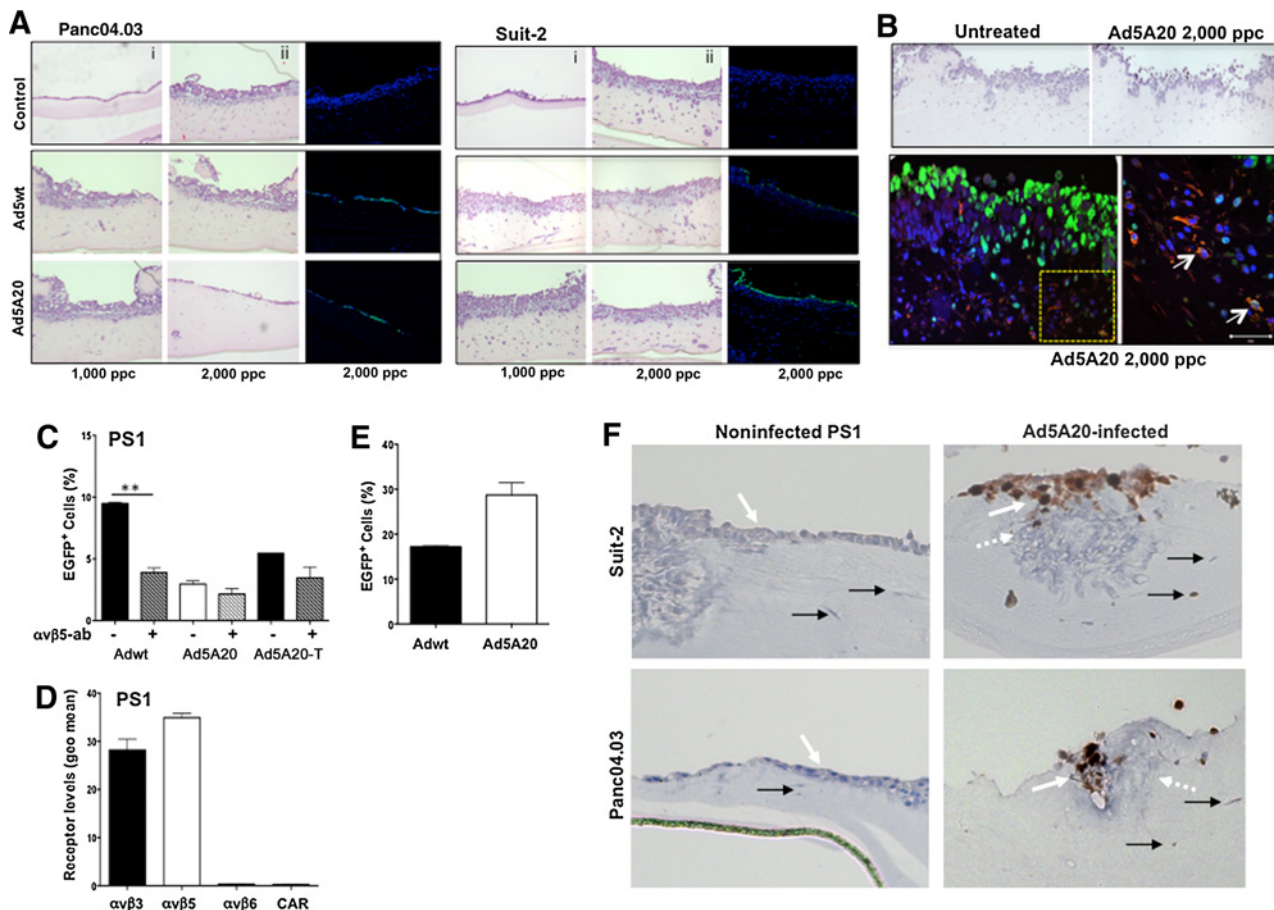
Cellular uptake of Ad5A20 and Ad5A20-477dITAYT is blocked by free A20FMDV2-peptide in cells expressing high levels of  $\alpha v\beta 6$  integrin. **A**, Expression profile of the integrin receptors ( $\alpha v\beta 3$ ,  $\alpha v\beta 5$ , and  $\alpha v\beta 6$ ) was determined in four selected pancreatic cancer cell lines. Relative expression levels were quantified by flow cytometry and represented by the geometric mean values,  $n = 3$ . \*,  $P < 0.001$  ( $\alpha v\beta 6$ ); °,  $P < 0.001$  ( $\alpha v\beta 5$ ), compared with levels in PT45. **B**, To verify  $\alpha v\beta 6$  integrin-mediated viral infection, the receptor was blocked with the  $\alpha v\beta 6$ -specific peptide (FMDVp; 10 nmol/L) prior to viral infection (100 ppc) and analyzed for EGFP expression 48 hours later.  $n = 3$ ; \*,  $P < 0.02$ ; \*\*,  $P < 0.01$ ,  $t$  test, two-tailed.

stellate cells as a major component promoting invasion and restricting delivery of drugs to the tumor (35, 36). To explore efficacy of the Ad5A20 and Ad5A20-477dITAYT mutants under conditions that are more similar to the tumor microenvironment than 2D monocultures, Panc04.03 or Suit-2 cells were cocultured with transformed nontumorigenic pancreatic stellate cells (PS1) in 3D collagen Matrigels (27–29). Growth of both cancer cell lines was greatly increased in the presence of PS1 cells, forming duct-like structures when seeded and cultured within the gels (Supplementary Fig. S2), as previously reported for organoids established from human and murine pancreatic tumor tissue (37–39). Panc04.03 or Suit-2 cells seeded together with PS1 cells on top of gel matrices formed thick epithelial layers with increased cellular invasion into the substrate (Fig. 4A, ii; top). However, in the absence of PS1 cells, the cancer cells mostly formed monolayers on top of the gels and did not invade the matrices (Fig. 4A, i). The 3D culture conditions were compatible with adenoviral propagation regardless of where the cells were seeded (Fig. 4A; Sup-

plementary Fig. S2). After 4 days of coculturing PS1 cells with Panc04.03 or Suit-2 cells, the addition of Ad5wt and Ad5A20 resulted in viral spread through multiple cell layers when cells were seeded on top of the gels. The thickness of the uppermost epithelial layers decreased with increased viral dose, demonstrating virus-dependent cell killing (Fig. 4A; middle and bottom). The cell killing was greatest with the Ad5A20 mutant in Panc04.03 cells with few remaining live E1A-positive cells 4 days after infection (Fig. 4A; confocal images). The effect was similar in Suit-2 cells, although the inhibition of invasion and growth was less than in Panc04.03 cells (Fig. 4A; right). Importantly, we demonstrate that the infected epithelial cells were in sufficiently close contact with the PS1 stromal cells for virus to spread through the matrix and infect both cancer and stromal cells (Fig. 4B).

Viral infection and replication in PS1 cells were initially determined in 2D monocultures (Fig. 4C). As expected for non-epithelial cells, the level of infection was poor with the highest levels for Ad5wt with <10% of cells expressing EGFP, and <5% for



**Figure 4.**

Efficient cell killing upon delivery of Ad5wt and Ad5A20, in 3-dimensional organotypic cultures consisting of pancreatic cancer and stromal cells (PS1). **A**, Panc04.03 or Suit-2 cells were seeded on top of a gel matrix consisting of collagen and Matrigel either alone (i) or cocultured (ii) with PS1 cells. The cocultured cells were infected at 1,000 and 2,000 ppc 4 days after seeding and fixed in formalin 4 days after infection, embedded in paraffin, sectioned and stained with H&E,  $\times 5$  magnification. For confocal imaging, cellular nuclei were detected with DAPI (blue) and antibodies for E1A (green). **B**, Ad5A20 infects both Panc04.03 and PS1 cells. Sections were stained with H&E (top) and for confocal imaging (bottom). PS1 cells were identified by  $\alpha$ -SMA expression (red) and the localization of virus identified by E1A expression (green). Nuclei were detected with DAPI (blue),  $\times 20$  magnification. Area demarcated in the yellow square is magnified in the right. Infected PS1 cells appear yellow (white arrows). One representative study is shown,  $n \geq 3$ . **C**, Infection of PS1 cells with Adwt, Ad5A20, and Ad5A20-477d/TAYT (1,000 ppc) was challenged by blocking with  $\alpha\beta 5$  integrin-specific antibody (clone PIF6, 10  $\mu\text{g}/\text{mL}$ ). EGFP-positive cells were detected by flow cytometry 72 hours postinfection. **D**, Relative expression levels of cell surface integrins  $\alpha\beta 3$ ,  $\alpha\beta 5$ ,  $\alpha\beta 6$ , and CAR in PS1 cells, quantified by flow cytometry,  $n = 3$ . **E**, PS1 cells were infected with Adwt or AdA20 (4,000 ppc) for 72 hours, virus-containing cell-free media were prepared, and 50  $\mu\text{L}$  was transferred to epithelial 2D monolayers. Panc04.03 cells were trypsinized 24 hours later and analyzed for EGFP expression by FACS,  $n = 3$ . **F**, PS1 cells were seeded on top of the gel; 24 hours later, cells were infected with AdA20 (2,000 ppc; right) or mock-treated (left). After 48 hours, the cultures were washed to remove noninternalized virus and Panc04.03 (bottom) or Suit-2 (top) cells were seeded on top of gels; 4 days later, the cultures were fixed and stained for E1A expression (brown) and H&E,  $\times 20$  magnification. Black arrows indicate noninfected (left) and infected (right) fibroblasts; white arrows indicate noninfected (left) and infected (right) epithelial cells; white dashed arrows point toward lysed or necrotic cells.

the retargeted mutants compared with 20% to 50% in  $\alpha\beta 6$  integrin-expressing epithelial cancer cells (Figs. 4C and 3B). Importantly, the early viral E1A gene was expressed at detectable levels in the PS1 monolayers (Supplementary Fig. S3A and S3B). Viral uptake was likely mediated by  $\alpha\beta 3$  and  $\alpha\beta 5$  integrins (Fig. 4D) and was significantly reduced in the presence of an anti- $\alpha\beta 5$  integrin antibody (Fig. 4C). CAR and the  $\alpha\beta 6$  integrin were not detected in PS1 cells (Fig. 4D). We tested whether viruses could be released from infected PS1 cells and spread to neighboring cancer cells. After infecting PS1 cells with Adwt or Ad5A20, following a 72-hour incubation period, the cell-free culture media were transferred to Panc04.03 and Suit-2 monolayers. Potent viral

infection and early gene expression was observed in both cancer cell lines (shown for Panc04.03; Fig. 4E). Viral spread was also confirmed in 3D cultures by a similar two-step process; PS1 cells preseeded onto matrices were infected with viruses and after removal of excess free virus (48 hours postinfection), noninfected Panc04.03 or Suit-2 cells were seeded on top. Sufficient virions were produced from the PS1 cells to infect and eliminate the majority of the cancer cells 72 hours postinfection (Fig. 4F). These findings collectively provide evidence that the retargeted adenoviral mutants infected both pancreatic stellate and cancer cells and could spread from cell-to-cell in the 3D culture system that represents the tumor microenvironment more accurately.

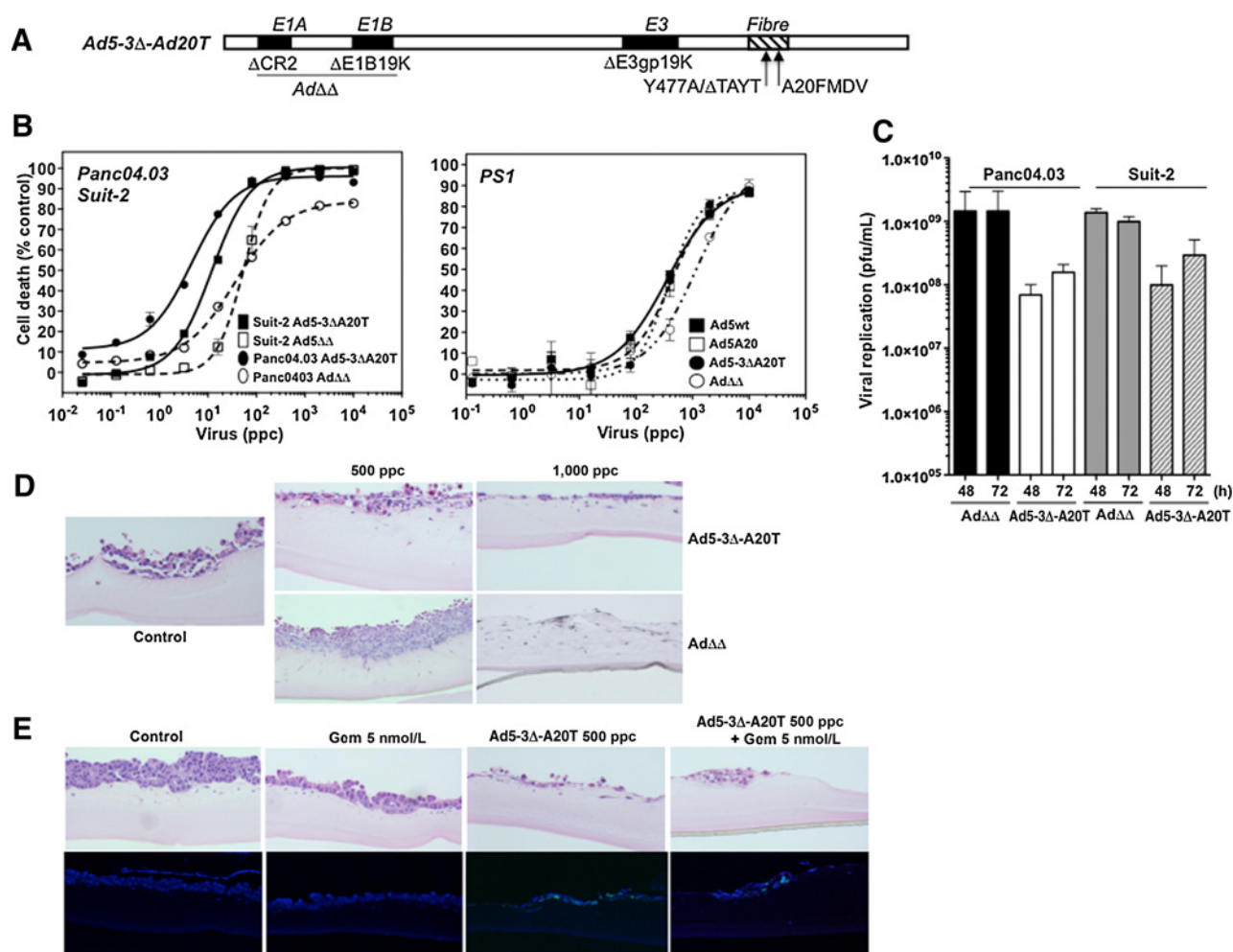


**Figure 5.**

The novel retargeted oncolytic mutant Ad5-3Δ-A20T potentially infects, replicates, and kills cocultured pancreatic cancer and stromal cells with and without gemcitabine. **A**, Schematic diagram of the modified Ad5-3Δ-A20T derived from the potent and replication-selective oncolytic mutant Ad5ΔΔ; for details, see text. **B**, Viral dose-response curves were generated (MTS-assay) to compare cell viability of Ad5ΔΔ against Ad5-3Δ-A20T in Panc04.03 and Suit-2 cells (left), and PS1 cells (right), 72 hours post infection. Representative study,  $n = 3$ . **C**, Viral replication determined by TCID<sub>50</sub> assay. Cells were infected with Ad5-3Δ-A20T or Ad5ΔΔ (100 ppc) for 48 and 72 hours and virus collected from media and cells and applied on JH293 cells for replication assay,  $n = 2$ . **D**, Panc04.03 cells cocultured with PS1 cells in 3D collagen/Matrigels. After 4 days, Ad5-3Δ-A20T was applied (top; 500–1,000 ppc) or Ad5ΔΔ (bottom; 500–1,000 ppc) in serum-free media from the top of the cultures, harvested 4 days after infection, and stained with H&E,  $\times 5$  magnification. **E**, Suit-2 cells cocultured with PS1 cells as above and 4 days after seeding infected with Ad5-3Δ-A20T at the indicated doses  $\pm$  gemcitabine at 5 nmol/L, representative images,  $n = 3$ . Cultures were harvested 4 days after infection and stained with H&E. Bottom, confocal images of the corresponding sections stained for DAPI (blue; nuclei) and E1A (green).

### The novel retargeted and replication-selective oncolytic mutant Ad5-3Δ-A20T is highly efficacious in pancreatic cancer cell lines

To further exploit the selective targeting to  $\alpha\beta 6$  integrins on pancreatic cancer cells, the A20FMDV2 peptide was inserted and CAR binding was ablated in the fiber knob (HI-loop) of the Ad5ΔΔ mutant, to generate Ad5-3Δ-A20T (Fig. 5A; Supplementary Fig. S1B; refs. 6, 23, 24). In addition to the E1ACR2 and E1B19K deletions in Ad5ΔΔ that provide replication selectivity and apoptosis enhancement, deletion of the TAYT motif and the point mutation at Y477A were included to reduce CAR binding. These mutations and the insertion of the A20FMDV2 peptide were identical to the alterations in the parental Ad5A20-477ΔTAYT mutant (Fig. 5A; Supplementary Fig. S1B; refs. 18,

24, 40). The resulting oncolytic mutant Ad5-3Δ-A20T killed Panc04.03 and Suit-2 cells more potently than the parental Ad5ΔΔ mutant demonstrated by 10- and 5-fold lower EC<sub>50</sub> values (Fig. 5B; left). In contrast, in PS1 cells that were significantly less sensitive to virus-induced cell killing ( $>10$ -fold higher EC<sub>50</sub> values), the novel mutant had similar cell killing potency as Ad5wt (Fig. 5B; right). Replication of Ad5-3Δ-A20T in Panc04.03 and Suit-2 cells was slightly less than for Ad5ΔΔ (Fig. 5C). Replication in PS1 cells was also less for Ad5-3Δ-A20T than for Ad5ΔΔ. However, both viruses showed  $>100$ -fold lower levels of replication in PS1 than in epithelial cells; Ad5-3Δ-A20T replication was  $4.2 \times 10^5 \pm 2.2 \times 10^5$  pfu/mL and Ad5ΔΔ  $1.7 \times 10^7 \pm 5.1 \times 10^6$  pfu/mL ( $n = 3$ ) 48 hours postinfection in the stromal cells.



### Ad5-3 $\Delta$ -A20T potently inhibits growth and invasion of Panc04.03 cells in 3D cocultures with the pancreatic stromal PS1 cells

Dose-dependent cell killing was observed when 3D cocultures of Panc04.03-PS1 cells were infected with Ad5-3 $\Delta$ -A20T or Ad $\Delta\Delta$  (500 and 1,000 ppc) for 4 days (Panc04.03; Fig. 5D). In cultures infected with Ad5-3 $\Delta$ -A20T, viable and/or invading cells appeared to be fewer than in Ad $\Delta\Delta$ -infected cultures at the lower dose, whereas the higher dose eliminated most cells with both viruses. Importantly, the efficacy of Ad5-3 $\Delta$ -A20T was retained in organotypic cocultures of Panc04.03 or Suit-2 with PS1 cells when treated simultaneously with gemcitabine (Suit-2; Fig. 5E; Supplementary Fig. S4). We previously demonstrated that both Ad $\Delta\Delta$  and Ad $\Delta$ 19K synergized with low doses of gemcitabine in pancreatic cancer cells in 2D monocultures and *in vivo*, including Suit-2 models, by enhancing apoptotic death through mitotic aberrations (11, 14). We found that the 3D coculture system was a suitable model for screening the efficacy of adenoviral mutants and for confirming compatibility with current therapeutic cytotoxic drugs.

### Ad5-3 $\Delta$ -A20T efficiently inhibits growth of human pancreatic cancer xenografts in murine models

The potent elimination of Panc04.03 and Suit-2 cells grown in 2D mono- and 3D cocultures was confirmed *in vivo*, using Suit-2 xenografts grown subcutaneously in athymic mice. We have previously demonstrated that the Suit-2 model is suitable for determining efficacy of adenoviral mutants administered alone or in combination with cytotoxic drugs (12, 41). Both Adwt and Ad5-3 $\Delta$ -A20T potently prevented tumor growth up to 20 days after the first administration of virus (Fig. 6A). From 20 to 42 days, growth was greatly reduced compared with the mock-treated animals that were culled already after 18 days due to tumor burden and ulcer formation. The median time to tumor progression was significantly prolonged ( $P < 0.0004$ ) from 11 days for mock-treated animals to 42 days with Ad5-3 $\Delta$ -A20T and 37 days for Adwt (Fig. 6B). Tumors harvested when animals were culled showed intense E1A expression for both viruses up to 53 days after virus administration (Fig. 6C). The ultimate goal of generating Ad5-3 $\Delta$ -A20T was to increase viral dose at tumor lesions after systemic delivery. In this proof-of-concept study, potent expression of E1A was observed in Suit-2 tumors after a single tail vein administration of Ad5-3 $\Delta$ -A20T (Fig. 6D). Interestingly, E1A expression appeared to be lower after tail vein injection with Adwt. The results from the 3D cocultures and the *in vivo* studies demonstrated that Ad5-3 $\Delta$ -A20T was at least as efficacious as Ad5wt under conditions that more realistically mimic the tumor microenvironment *in situ* in patients. Future studies will be aimed at quantifying the retargeting efficacy in murine models that can mimic the conditions in patients more accurately including systems with humanized blood factors. Taken together, our data support further exploration of Ad5-3 $\Delta$ -A20T for potential future development into novel anti-cancer agents targeting pancreatic cancer.

## Discussion

No curative treatments are currently available for patients with metastatic PDAC, and resistance to chemotherapeutics inevitably develops. The recent identification of several biomarkers will hopefully enable earlier detection and curative

surgery in more patients (42, 43). In contrast, replication-selective oncolytic adenoviral mutants target pancreatic cancer at any stage by direct oncolysis, reversal of drug resistance, and activation of antitumor immune responses but have poor efficacy when delivered systemically (8, 10). The focus of our study was to optimize the potent and selective oncolytic mutant Ad $\Delta\Delta$  (6) to enable future development of this mutant for systemic delivery by taking advantage of the selective expression of  $\alpha\text{v}\beta 6$  integrin in pancreatic cancer cells. We generated the replication-selective integrin-targeted Ad5-3 $\Delta$ -A20T mutant expressing the small  $\alpha\text{v}\beta 6$ -peptide ligand A20FMDV2. The A20FMDV2 peptide was derived from the GH-loop in VP1 in the capsid of the FMDV and is essential for infection in cloven-hoofed animals (44). The affinity to  $\alpha\text{v}\beta 6$  integrins was high, measured at  $K_D = 0.22$  nmol/L, whereas binding to other integrins, including  $\alpha\text{v}\beta 3$ ,  $\alpha\text{v}\beta 5$ , and  $\alpha\text{v}\beta 1$ , was more than 80-fold lower (21, 25). The selective binding to  $\alpha\text{v}\beta 6$  integrins was shown to be dependent on the DLXXL motif in the carboxy  $\alpha$ -helical loop next to the RGD domain at the apex of the loop domain in the peptide (23, 26, 44, 45).

We previously demonstrated that the retargeted wild-type mutants Ad5A20 and Ad5A20-477dITAYT infected breast and ovarian carcinoma cells expressing the  $\alpha\text{v}\beta 6$  integrin (23, 24). In the current study, we demonstrated that infection with these mutants strongly correlated with  $\alpha\text{v}\beta 6$  integrin levels in a panel of 15 PDAC cell lines. In two cell lines that express relatively high levels of  $\alpha\text{v}\beta 6$  integrins (CFPAC-1 and Capan-2), lower than expected levels of infection with the retargeted mutants were observed. In the same cell lines, lower infection levels were demonstrated with Ad5wt, which overall suggest that these cells are generally insensitive to viral infection and/or viral gene expression. Correspondingly, transduction of CFPAC-1 cells with native Ad5, expressing a reporter gene, was demonstrated to be less efficient than of MIA PaCa-2, PANC-1, and BxPC-3 cells (46). Infectivity was monitored by viral EGFP expression, which in turn was regulated by the early viral E1A gene product, suggesting that both retargeted mutants entered the early endosomes even when attachment was through the  $\alpha\text{v}\beta 6$  integrin rather than CAR. The classical route of internalization of native Ad5 is via fiber knob binding to CAR on epithelial cells, which initiates binding of penton base proteins to  $\alpha\text{v}\beta 3$  and  $\alpha\text{v}\beta 5$  integrins through RGD motifs, activating clathrin-mediated endocytosis (47). Acidification of the virus-containing endosome is required for release of viral genomes and proteins into the cytosol and for transport into the nucleus and completion of the viral life cycle. The level of infection by the retargeted mutants correlated with expression levels of the  $\alpha\text{v}\beta 6$  integrins and was reflected in the degree of cell killing in all the selected cell lines except BxPC-3. This cell line expressed all the tested integrins ( $\alpha\text{v}\beta 3$ ,  $\alpha\text{v}\beta 5$ , and  $\alpha\text{v}\beta 6$ ) and CAR. The presence of these receptors likely contributed to the high sensitivity to Adwt infection producing the lowest EC<sub>50</sub> values of all tested cell lines allowing for only small differences in cell killing ability between Adwt and the retargeted mutants. It is interesting to note that both Panc04.03 and Suit-2 have low levels of CAR and the  $\alpha\text{v}\beta 3$  integrin and the highest levels of  $\alpha\text{v}\beta 6$  integrin expression, the reverse of the BxPC-3 cells.

To further support the notion that our retargeted mutants likely internalize and infect in a similar way to wild-type virus, we showed that total viral genome amplification paralleled the levels of infectivity, whereas the rate of replication remained similar to

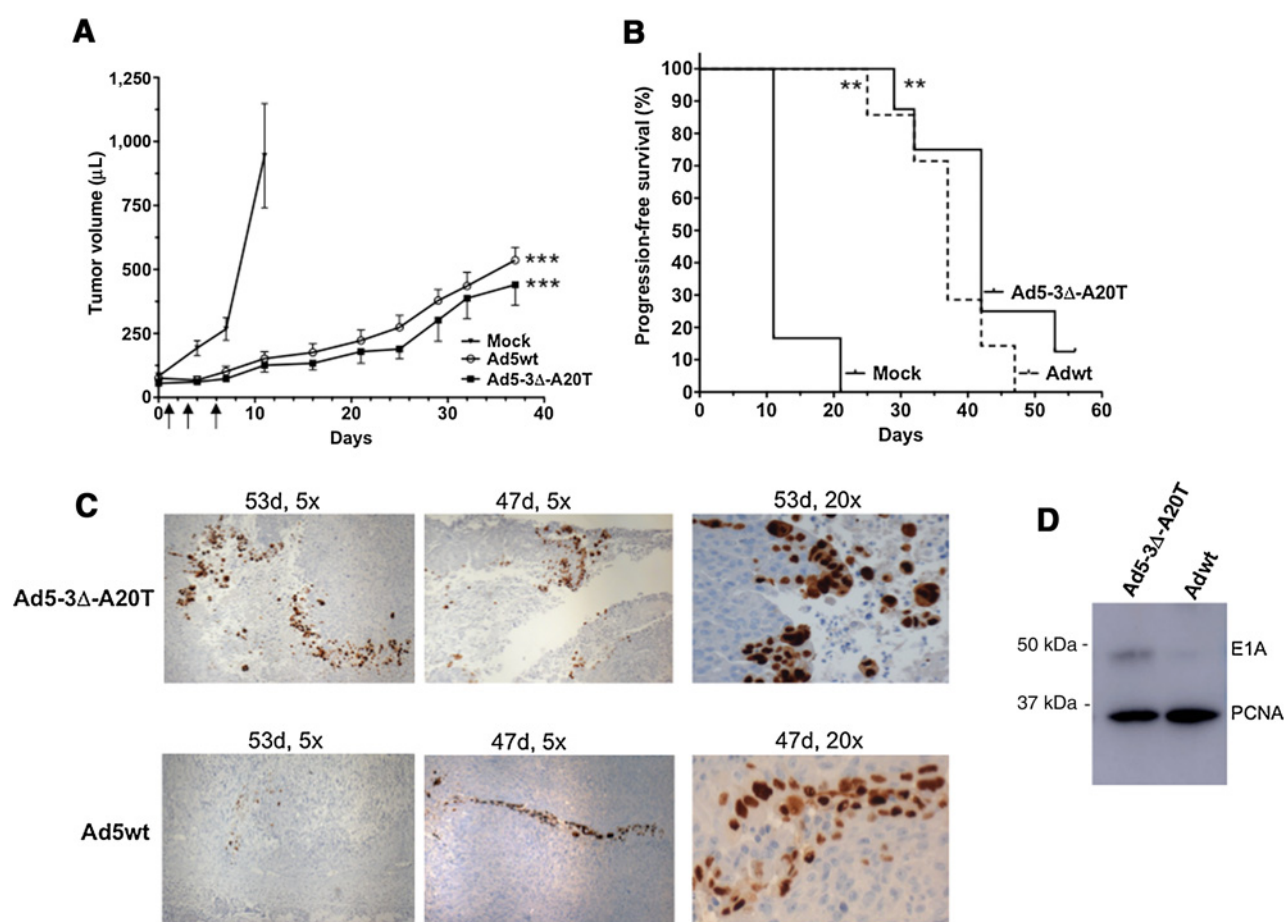


**Figure 6.**

Ad5-3Δ-A20T inhibits growth of Suit-2 tumor xenografts in athymic mice. **A**, Suit-2 cells ( $1 \times 10^6$  cells) were inoculated subcutaneously in one flank of CDnu/nu athymic mice. Adenoviral mutants or PBS (mock controls) were administered intratumorally ( $3 \times 10^9$  vp/injection) on days 1, 3, and 6 (arrows), when tumors had reached  $100 \pm 20$   $\mu$ L (14 days after inoculation). Tumor growth was determined until tumors reached 1.44 cm<sup>2</sup>. One-way ANOVA, \*\*\*,  $P < 0.001$  compared with mock, 8 animals per group. **B**, Kaplan-Meier survival curves generated from time to tumor progression set at 500  $\mu$ L. \*\*,  $P < 0.01$  compared with mock,  $n = 8$ . **C**, Tissue sections from tumors harvested at the end of the study, stained for E1A expression by IHC, representative tumor images ( $\times 5$  and  $\times 20$  magnification as shown). **D**, Detection of E1A viral protein in Suit-2 tumor lysates from animals administered a single tail vein injection ( $3 \times 10^9$  vp/100  $\mu$ L) with the respective virus. Animals were treated when tumor volumes reached  $120 \pm 30$  mm<sup>3</sup> in size. Tumors were excised and sonicated 72 hours later for immunoblotting analysis, one representative study from two animals, 20  $\mu$ g total protein/lane.

that of Ad5wt in each cell line. Thus, viral propagation was not hampered by the retargeted fibers and nuclear entry of the viral genome could proceed. Internalization of the retargeted mutants via  $\alpha\beta 6$  integrin was confirmed by blocking infection with free A20FMDV2 peptide. Intracellular processing of the FMDV virus is less established, but includes a pathway similar to that of Ad5, with additional intracellular mechanisms implicated (48). It was recently reported that binding of the A20FMDV2 peptide alone to normal human bronchial epithelial (NHBE) cells caused rapid internalization of the peptide- $\alpha\beta 6$  integrin complex in endosomes, although the postinternalization events were suggested to be more complex with partial delay of recycling of the integrin to the cell surface (25). Nevertheless, our  $\alpha\beta 6$  integrin-retargeted Ad5 mutants infected and replicated to similar levels as Adwt in PDAC cells. The exact cellular factors involved in the internalization, endocytosis, nuclear transport, or the rate of cellular processing may differ for viruses internalized via  $\alpha\beta 6$  compared with  $\alpha\beta 3$  and  $\alpha\beta 5$  integrins. Interestingly, pancreatic stellate

cells that lack  $\alpha\beta 6$  integrins were infected by Ad5-3Δ-A20T, suggesting that uptake in these cells was dependent on other integrins, including  $\alpha\beta 5$ , in the presence of high local doses of virus. These processes are the subjects for future investigations.

Following the initial proof-of-concept studies, the chimeric fiber from Ad5A20-477dITAYT was engineered into the AdΔΔ mutant to generate Ad5-3Δ-A20T. The additional modifications to the CAR-binding region of the fiber knob were also retained as a strategy to facilitate systemic delivery in future studies. We previously found that Ad5A20-477dITAYT had improved liver-to-tumor viral genome ratios possibly through abrogation of FIX/C4BP binding due to the TAYT deletion (18, 24). Importantly, Ad5A20-477dITAYT did not agglutinate erythrocytes due to detargeting of CAR through the Y477A mutation. The novel Ad5-3Δ-A20T mutant infected and killed  $\alpha\beta 6$  integrin expressing PDAC cells more efficiently than both Ad5wt and the parental AdΔΔ mutant. Viral functions, including infection, gene expression, and viral replication, were retained,

supporting propagation in all tested cell lines. However, replication was slightly lower with the new mutant than with Ad $\Delta\Delta$ , indicating that the increased viral uptake and consequently, early viral gene expression, initiated cell killing before maximal number of virions were produced, as previously demonstrated in NHBE cells and PDAC cells treated with viral replication inhibitors (12). Furthermore, Ad5-3 $\Delta$ -A20T had approximately a 4-fold higher vp/pfu ratio compared with Adwt or Ad $\Delta\Delta$ , although production in A549 cells resulted in similar yields of viral particles for all three viruses. Nevertheless, Ad5-3 $\Delta$ -A20T was as potent as Ad5wt in tumor xenograft models in athymic mice. When injected intratumorally, the retargeted mutant spread within the solid tumors similar to Ad5wt and as previously reported for Ad $\Delta\Delta$  (6). Complete elimination of tumors was not possible with either Ad5-3 $\Delta$ -A20T or Ad5wt because of limitations of the *in vivo* model. Murine tissues do not support productive infection with human adenovirus, preventing spread within the murine tumor microenvironment in addition to the rapid xenograft growth and the absence of an immune response (49). Despite the rapid hepatic elimination of adenovirus in mice, we confirmed that intravenous delivery of Ad5-3 $\Delta$ -A20T resulted in high levels of viral gene expression in Suit-2 tumors. Future studies will address whether the retargeted mutant will reach tumors in sufficiently high levels to warrant systemic administration. Importantly, the Suit-2 cells employed in the xenograft studies expressed lower levels of  $\alpha v \beta 6$  integrin and higher levels of  $\alpha v \beta 5$  compared with Panc04.03 cells. We predict that tumor xenografts with similar integrin profiles, high  $\alpha v \beta 6$ , and lower  $\alpha v \beta 3$  and  $\alpha v \beta 5$  integrin expression would reflect the higher cell killing seen *in vitro*.

We optimized the previously developed 3D coculture models of pancreatic stellate and cancer cell lines (27–29), for investigating viral infection and spread in this study. These models have more similarities with the tumor microenvironment in patients than traditional 2D monocultures. In addition, the interaction with human stromal cells is retained without interference from murine stroma present in athymic mice models. Although more sophisticated organoid culture models have been described for murine and patient tumor tissue including a few methods for modeling pancreatic cancer (37, 39), we found that our 3D cocultures were more suitable for screening of viral functions. We found that both Ad5-3 $\Delta$ -A20T and Ad5A20 were more efficacious than Ad5wt and Ad $\Delta\Delta$  in infecting and eliminating Panc04.03 and Suit-2 cells, whereas in the murine models, the novel retargeted Ad5-3 $\Delta$ -A20T had similar efficacy to Adwt. The collagen-Matrigel matrices are likely to provide a more penetrable milieu for viral infectivity and spread than in dense murine stroma, further facilitating the enhanced infectivity of Ad5-3 $\Delta$ -A20T as demonstrated in the 2D cultures. We showed that human stellate cells (PS1) support viral infection and replication, albeit at significantly lower levels than pancreatic cancer cells, which could further augment viral spread within the cultures, in contrast to the murine test model. Our data demonstrate that viral efficacy was retained in the 3D cultures when Ad5-3 $\Delta$ -A20T was combined with low doses of gemcitabine. The deletion of the E1B19K gene causes enhancement of gemcitabine-dependent apoptosis, previously demonstrated for Ad $\Delta\Delta$  in PDAC cells (6, 11, 12, 14). We propose that the 3D cocultures are suitable model systems for investigating oncolytic virus replication and spread in the

presence of the multiple cell types that constitute the tumor microenvironment in patients. The flexibility of the system is achieved by varying the cell and matrix compositions; and treatment with viruses and/or drugs can be administered via different compartments to enable a tailored test system appropriate for the research question. In conclusion, the 3D cultures complement the limitations of 2D cell cultures and murine *in vivo* models by providing a suitable platform for selecting the best viral mutant candidates to pursue clinically.

Herein, we provide evidence that the complex alterations of the viral genome in the novel selective Ad5-3 $\Delta$ -A20T mutant did not compromise viral functions in  $\alpha v \beta 6$  integrin expressing PDAC cells but rather enhanced infectivity and cell killing selectively, in these cells. In addition to the E1ACR2 and E1B19K deletions for replication selectivity and apoptosis enhancement in Ad $\Delta\Delta$ , the E3gp19K gene was deleted to increase recruitment of immune cells to infected tumor cells with the aim to enhance efficacy in future clinical applications. We consider Ad5-3 $\Delta$ -A20T an excellent candidate for targeting pancreatic cancer. Further biodistribution studies will elucidate whether additional modifications are necessary to eliminate tumors after systemic delivery, for example, by introducing modifications to avoid neutralizing antibodies and/or hepatic elimination. Our results may open new avenues for improving the delivery and efficacy of potent oncolytic adenoviral mutants in patients with pancreatic cancer.

#### Disclosure of Potential Conflicts of Interest

No potential conflicts of interest were disclosed.

#### Authors' Contributions

**Conception and design:** Y.K.S. Man, J.A. Davies, J.F. Marshall, A.L. Parker, G. Halldén

**Development of methodology:** Y.K.S. Man, J.A. Davies, L. Coughlan, A. Blázquez-Moreno, A.L. Parker, G. Halldén

**Acquisition of data (provided animals, acquired and managed patients, provided facilities, etc.):** Y.K.S. Man, J.A. Davies, L. Coughlan, C. Pantelidou, G. Halldén

**Analysis and interpretation of data (e.g., statistical analysis, biostatistics, computational analysis):** Y.K.S. Man, C. Pantelidou, A. Blázquez-Moreno, A.L. Parker, G. Halldén

**Writing, review, and/or revision of the manuscript:** Y.K.S. Man, J.A. Davies, J.F. Marshall, A.L. Parker, G. Halldén

**Administrative, technical, or material support (i.e., reporting or organizing data, constructing databases):** Y.K.S. Man, G. Halldén

**Study supervision:** A.L. Parker, G. Halldén

#### Acknowledgments

This study was supported by generous grants from the UK Charity Pancreatic Cancer Research Fund (PCRF), the BCI CRUK Centre Grant (grant number C16420/A18066; to G. Halldén, Y.K.S. Man, and C. Pantelidou), and the CRUK Biotherapeutics Drug Discovery Project Award (grant number 23946; to A.L. Parker and J.A. Davies). We want to thank Dr. Elisabete Carapuca for expert suggestions on IHC and confocal microscopy, and Professor Hemant Kocher for the kind gift of PS1 cells and helpful discussions and advice. We greatly appreciate the excellent assistance by Julie Andow, Tracy Chaplin-Perkins, and Hagen Schmidt.

The costs of publication of this article were defrayed in part by the payment of page charges. This article must therefore be hereby marked *advertisement* in accordance with 18 U.S.C. Section 1734 solely to indicate this fact.

Received July 13, 2017; revised September 27, 2017; accepted November 30, 2017; published OnlineFirst January 24, 2018.

## References

- Oettle H. Progress in the knowledge and treatment of advanced pancreatic cancer: from benchside to bedside. *Cancer Treat Rev* 2014; 40:1039–47.
- Kulke MH, Tempero MA, Niedzwiecki D, Hollis DR, Kindler HL, Cusnir M, et al. Randomized phase II study of gemcitabine administered at a fixed dose rate or in combination with cisplatin, docetaxel, or irinotecan in patients with metastatic pancreatic cancer: CALGB 89904. *J Clin Oncol* 2009;27:5506–12.
- Hecht JR, Bedford R, Abbruzzese JL, Lahoti S, Reid TR, Soetikno RM, et al. A phase I/II trial of intratumoral endoscopic ultrasound injection of ONYX-015 with intravenous gemcitabine in unresectable pancreatic carcinoma. *Clin Cancer Res* 2003;9:555–61.
- Mulvihill S, Warren R, Venook A, Adler A, Randlev B, Heise C, et al. Safety and feasibility of injection with an E1B-55 kDa gene-deleted, replication-selective adenovirus (ONYX-015) into primary carcinomas of the pancreas: a phase I trial. *Gene Ther* 2001;8:308–15.
- O'Shea CC, Johnson L, Bagus B, Choi S, Nicholas C, Shen A, et al. Late viral RNA export, rather than p53 inactivation, determines ONYX-015 tumor selectivity. *Cancer Cell* 2004;6:611–23.
- Öberg D, Yanover E, Sweeney K, Adam V, Costas C, Lemoine NR, et al. Improved potency and selectivity of an oncolytic E1ACR2 and E1B19K deleted adenoviral mutant (AdΔΔ) in prostate and pancreatic cancers. *Clin Cancer Res* 2010;16:541–53.
- Raki M, Kanerva A, Ristimäki A, Desmond RA, Chen DT, Ranki T, et al. Combination of gemcitabine and Ad5/3-Delta24, a tropism modified conditionally replicating adenovirus, for the treatment of ovarian cancer. *Gene Ther* 2005;12:1198–205.
- Jiang H, Clise-Dwyer K, Ruisaard KE, Fan X, Tian W, Gumin J, et al. Delta-24-RGD oncolytic adenovirus elicits anti-glioma immunity in an immunocompetent mouse model. *PLoS One* 2014;9:e97407.
- Jones S, Zhang X, Parsons DW, Lin JC, Leary RJ, Angenendt P, et al. Core signaling pathways in human pancreatic cancers revealed by global genomic analyses. *Science* 2008;321:1801–6.
- Martinez-Velez N, Xipell E, Jauregui P, Zalacain M, Marrodan L, Zanduetta C, et al. The oncolytic adenovirus Delta24-RGD in combination with cisplatin exerts a potent anti-osteosarcoma activity. *J Bone Miner Res* 2014;29:2287–96.
- Cherubini G, Kallin C, Mozetic A, Hammaren-Busch K, Muller H, Lemoine NR, et al. The oncolytic adenovirus AdDeltaDelta enhances selective cancer cell killing in combination with DNA-damaging drugs in pancreatic cancer models. *Gene Ther* 2011;18:1157–65.
- Leitner S, Sweeney K, Öberg D, Davies D, Miranda E, Lemoine NR, et al. Oncolytic adenoviral mutants with E1B19K gene deletions enhance gemcitabine-induced apoptosis in pancreatic carcinoma cells and anti-tumor efficacy in vivo. *Clin Cancer Res* 2009;15:1730–40.
- White E. Mechanisms of apoptosis regulation by viral oncogenes in infection and tumorigenesis. *Cell Death Differ* 2006;13:1371–7.
- Pantelidou C, Cherubini G, Lemoine NR, Hallden G. The E1B19K-deleted oncolytic adenovirus mutant AdDelta19K sensitizes pancreatic cancer cells to drug-induced DNA-damage by down-regulating Claspain and Mre11. *Oncotarget* 2016;7:15703–24.
- Carlisle RC, Di Y, Cerny AM, Sonnen AF, Sim RB, Green NK, et al. Human erythrocytes bind and inactivate type 5 adenovirus by presenting Cocksackie virus-adenovirus receptor and complement receptor 1. *Blood* 2009;113:1909–18.
- Jonsson MI, Lenman AE, Frangmyr L, Nyberg C, Abdullahi M, Arnberg N. Coagulation factors IX and X enhance binding and infection of adenovirus types 5 and 31 in human epithelial cells. *J Virol* 2009;83:1816–25.
- Kalyuzhnyi O, Di Paolo NC, Silvestry M, Hofherr SE, Barry MA, Stewart PL, et al. Adenovirus serotype 5 hexon is critical for virus infection of hepatocytes *in vivo*. *Proc Natl Acad Sci U S A* 2008;105:5483–8.
- Shayakhmetov DM, Gaggari A, Ni S, Li ZY, Lieber A. Adenovirus binding to blood factors results in liver cell infection and hepatotoxicity. *J Virol* 2005;79:7478–91.
- Doronin K, Flatt JW, Di Paolo NC, Khare R, Kalyuzhnyi O, Accchione M, et al. Coagulation factor X activates innate immunity to human species C adenovirus. *Science* 2012;338:795–8.
- Bates RC, Bellovin DI, Brown C, Maynard E, Wu B, Kawakatsu H, et al. Transcriptional activation of integrin beta6 during the epithelial-mesenchymal transition defines a novel prognostic indicator of aggressive colon carcinoma. *J Clin Invest* 2005;115:339–47.
- Hausner SH, Abbey CK, Bold RJ, Gagnon MK, Marik J, Marshall JF, et al. Targeted *in vivo* imaging of integrin alphavbeta6 with an improved radiotracer and its relevance in a pancreatic tumor model. *Cancer Res* 2009;69:5843–50.
- Allen MD, Thomas GJ, Clark S, Dawoud MM, Vallath S, Payne SJ, et al. Altered microenvironment promotes progression of preinvasive breast cancer: myoepithelial expression of alphavbeta6 integrin in DCIS identifies high-risk patients and predicts recurrence. *Clin Cancer Res* 2014;20:344–57.
- Coughlan L, Vallath S, Saha A, Flak M, McNeish IA, Vassaux G, et al. *In vivo* retargeting of adenovirus type 5 to alphavbeta6 integrin results in reduced hepatotoxicity and improved tumor uptake following systemic delivery. *J Virol* 2009;83:6416–28.
- Coughlan L, Vallath S, Gros A, Gimenez-Alejandre M, Van Rooijen N, Thomas GJ, et al. Combined fiber modifications both to target alpha(v) beta(6) and detarget the coxsackievirus-adenovirus receptor improve virus toxicity profiles *in vivo* but fail to improve antitumoral efficacy relative to adenovirus serotype 5. *Hum Gene Ther* 2012;23:960–79.
- Slack RJ, Hafeji M, Rogers R, Ludbrook SB, Marshall JF, Flint DJ, et al. Pharmacological characterization of the alphavbeta6 integrin binding and internalization kinetics of the foot-and-mouth disease virus derived peptide A20FMDV2. *Pharmacology* 2016;97:114–25.
- Dicara D, Burman A, Clark S, Berryman S, Howard MJ, Hart IR, et al. Foot-and-mouth disease virus forms a highly stable, EDTA-resistant complex with its principal receptor, integrin alphavbeta6: implications for infectiousness. *J Virol* 2008;82:1537–46.
- Froeling FE, Mirza TA, Feakins RM, Seedhar A, Elia G, Hart IR, et al. Organotypic culture model of pancreatic cancer demonstrates that stromal cells modulate E-cadherin, beta-catenin, and Ezrin expression in tumor cells. *Am J Pathol* 2009;175:636–48.
- Coleman SJ, Chioni AM, Ghallab M, Anderson RK, Lemoine NR, Kocher HM, et al. Nuclear translocation of FGF1 and FGF2 in pancreatic stellate cells facilitates pancreatic cancer cell invasion. *EMBO Mol Med* 2014; 6:467–81.
- Carapuca EF, Gemenetzidis E, Feig C, Bapiro TE, Williams MD, Wilson AS, et al. Anti-stromal treatment together with chemotherapy targets multiple signalling pathways in pancreatic adenocarcinoma. *J Pathol* 2016;239: 286–96.
- Jackson T, Sheppard D, Denyer M, Blakemore W, King AM. The epithelial integrin alphavbeta6 is a receptor for foot-and-mouth disease virus. *J Virol* 2000;74:4949–56.
- Merron A, Peerlinck I, Martin-Duque P, Burnet J, Quintanilla M, Mather S, et al. SPECT/CT imaging of oncolytic adenovirus propagation in tumours *in vivo* using the Na/I symporter as a reporter gene. *Gene Ther* 2007; 14:1731–8.
- Warming S, Costantino N, Court DL, Jenkins NA, Copeland NG. Simple and highly efficient BAC recombineering using galK selection. *Nucleic Acids Res* 2005;33:e36.
- Stanton RJ, McSharry BP, Armstrong M, Tomasec P, Wilkinson GW. Re-engineering adenovirus vector systems to enable high-throughput analyses of gene function. *BioTechniques* 2008;45:659–62.
- Hezel AF, Deshpande V, Zimmermann SM, Contino G, Alagesan B, O'Dell MR, et al. TGF-beta and alphavbeta6 integrin act in a common pathway to suppress pancreatic cancer progression. *Cancer Res* 2012;72:4840–5.
- Froeling FE, Marshall JF, Kocher HM. Pancreatic cancer organotypic cultures. *J Biotechnol* 2010;148:16–23.
- Coleman SJ, Watt J, Arumugam P, Solaini L, Carapuca E, Ghallab M, et al. Pancreatic cancer organotypics: high throughput, preclinical models for pharmacological agent evaluation. *World J Gastroenterol* 2014;20:8471–81.
- Boj SF, Hwang CI, Baker LA, Chio II, Engle DD, Corbo V, et al. Organoid models of human and mouse ductal pancreatic cancer. *Cell* 2015;160: 324–38.
- Ohlund D, Handly-Santana A, Biffi G, Elyada E, Almeida AS, Ponz-Sarvisse M, et al. Distinct populations of inflammatory fibroblasts and myofibroblasts in pancreatic cancer. *J Exp Med* 2017;214:579–96.
- Baker LA, Tiriach H, Clevers H, Tuveson DA. Modeling pancreatic cancer with organoids. *Trends Cancer* 2016;2:176–90.

40. Kirby I, Davison E, Bevil AJ, Soh CP, Wickham TJ, Roelvink PW, et al. Mutations in the DG loop of adenovirus type 5 fiber knob protein abolish high-affinity binding to its cellular receptor CAR. *J Virol* 1999;73:9508–14.
41. Bhattacharyya M, Francis J, Eddouadi A, Lemoine NR, Hallden G. An oncolytic adenovirus defective in pRb-binding (dl922-947) can efficiently eliminate pancreatic cancer cells and tumors *in vivo* in combination with 5-FU or gemcitabine. *Cancer Gene Ther* 2011;18:734–43.
42. Radon TP, Massat NJ, Jones R, Alrawashdeh W, Dumartin L, Ennis D, et al. Identification of a three-biomarker panel in urine for early detection of pancreatic adenocarcinoma. *Clin Cancer Res* 2015;21:3512–21.
43. Debernardi S, Massat NJ, Radon TP, Sangaralingam A, Banissi A, Ennis DP, et al. Noninvasive urinary miRNA biomarkers for early detection of pancreatic adenocarcinoma. *Am J Cancer Res* 2015;5:3455–66.
44. Berryman S, Clark S, Kakker NK, Silk R, Seago J, Wadsworth J, et al. Positively charged residues at the five-fold symmetry axis of cell culture-adapted foot-and-mouth disease virus permit novel receptor interactions. *J Virol* 2013;87:8735–44.
45. DiCara D, Rapisarda C, Sutcliffe JL, Violette SM, Weinreb PH, Hart IR, et al. Structure-function analysis of Arg-Gly-Asp helix motifs in alpha v beta 6 integrin ligands. *J Biol Chem* 2007;282:9657–65.
46. Bouvet M, Bold RJ, Lee J, Evans DB, Abbruzzese JL, Chiao PJ, et al. Adenovirus-mediated wild-type p53 tumor suppressor gene therapy induces apoptosis and suppresses growth of human pancreatic cancer. *Ann Surg Oncol* 1998;5:681–8.
47. Meier O, Greber UF. Adenovirus endocytosis. *J Gene Med* 2004;6 Suppl 1: S152–63.
48. Miller LC, Blakemore W, Sheppard D, Atakilit A, King AM, Jackson T. Role of the cytoplasmic domain of the beta-subunit of integrin alpha(v) beta6 in infection by foot-and-mouth disease virus. *J Virol* 2001;75: 4158–64.
49. Cheong SC, Wang Y, Meng JH, Hill R, Sweeney K, Kim D, et al. E1A-expressing adenoviral E3B mutants act synergistically with chemotherapeutics in immunocompetent tumor models. *Cancer Gene Ther* 2008; 15:40–50.